

# AN ALGORITHM FOR FAULT DIAGNOSIS OF ATTITUDE AND ORBIT CONTROL SYSTEMS IN THE PRESENCE OF UNCERTAINTIES

**Alexandre Carvalho Leite, alexandre@cefetcampos.br**

CEFET Campos, Rua Doutor Siqueira, 273, Parque Dom Bosco, Campos RJ

**Marcelo Lopes de Oliveira Souza, marcelo@dem.inpe.br**

INPE, Avenida dos Astronautas, 1758, Jardim da Granja, São José dos Campos SP

**Abstract.** *In this work an algorithm for Fault Diagnosis of Attitude and Orbit Control Systems (AOCS) in the presence of uncertainties is presented. This includes: Fault Models, Residuals Generation, Signal Detection by means of Sequential Tests, and Diagnosis using Structured Hypothesis Tests. The faulty environment was simulated with abrupt, incipient and intermittent fault behaviors. Adaptive Thresholds were necessary to achieve robustness due to uncertainties in sensors, actuators and plant. Some tests conducted so far have shown the correctness of the algorithm in generating speculative Diagnosis Statements. After validating it, we intend to extend the algorithm to the AOCS of the MultiMission Platform (MMP) Satellite at the nominal operation mode. This is an excellent example of the engineering required to promote the interaction between universities and enterprises in the future.*

**Keywords:** *Fault Detection, Fault Diagnosis, Attitude and Orbit Control, Structured Hypothesis Tests, Sequential Probability Ratio Test.*

## 1. INTRODUCTION

The MMP was designed to have compatibility with small launchers. His total nominal mass is approximately 250 kilograms and its volume 2.81 cubic meters, including all subsystems. This work presents the design strategy used to develop a supervisor for the Attitude and Orbit Control System (AOCS) of the MMP Satellite. The focus of the supervisor is on Fault Detection and Diagnosis (FDD), but not yet reaching Fault Accommodation (FA) and Fault-Tolerant Control (FTC) - the handling of faults by means of redundancy and control law reconfiguration.

A previous work, [3], presented a new approach to examine faults in control systems in a systematic manner. But this previous work concerned itself with a general design strategy covering from fault detection to fault-tolerant control.

The problem consists in detecting and diagnosing faults in actuators and sensors of the MMP AOCS during a pointing maneuver around the pitch angle axis, in its Nominal Operating Mode. The achievement of the maneuver specifications is not of concern here.

Given this problem statement, the design strategy described in [3] is applied with some simplifications. The proposed algorithm is illustrated by application to the AOCS of the MMP Satellite. The concept, is however, suitable to other AOCS FDDS.

## 2. FDDS Design Methodology

The algorithms that realize FDD are a source of risk for faults (in the software) according to [2]. It implies that the overall reliability can only be improved if the FDD System (FDDS) is absolutely trustworthy. A search of an absolutely trustworthy FDDS could lead to a case of Russell's Paradox. But [3] introduces a seven-step design procedure that leads to an improved FDDS compared to what is obtainable by conventional ad-hoc methods.

A short summary of these design steps follows below:

1. A Failure Modes, Effects and Criticality Analysis (FMECA) of all involved sub-systems is performed and combined into a complete analysis of the entire satellite.
2. The top-level end-effects are judged for severity, and the ones with significant influence on the control performance are selected to be handled by the supervisor.
3. The possibilities of fault accommodation are considered.
4. A reverse deduction of FMECA rule base is performed down to the point of reconfiguration (step 3) to locate the faults that cause the considered end-effects.
5. FDD algorithms are designed based on measurements and control signals.
6. Fault accommodation actions are designed.

7. The most appropriate action is determined for fault accommodation.

Figure 1 shows this seven-step design procedure and relationship among all seven steps.

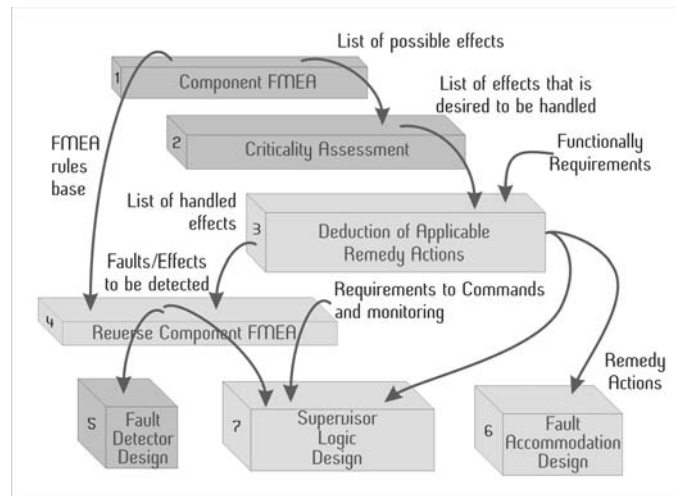


Figure 1. Systematic supervisor design approach adopted. Figure adapted from [3]

The purpose of this work, as mentioned, is on FDDS development only. Due to this specific purpose, the seven-step procedure will be reduced to a three-step procedure (dark gray boxes in figure 1), using only the steps 1, 2 and 5 above.

The main idea is to detect and diagnose faults in the AOCS of the MMP based on the information available in the measurements. This new three-step procedure compiles steps 1 and 2 of Figure 1 on a single new 1<sup>st</sup> step, and divides step 5 onto two new 2<sup>nd</sup> and 3<sup>rd</sup> steps. The whole three-step procedure for systematic fault diagnosis system design can be summarized as follows:

**Input:** The input is a 4-tuple  $\langle \Xi, M, \Phi_m, \Delta \rangle$ , where  $\Xi$  is a set of measurement data,  $M$  is a mathematical model which describes the nominal mode behavior present in  $\Xi$ ,  $\Phi_m$  is a set of fault modes candidates, and  $\Delta$  is a set of hypothesis test candidates.

**Step 1:** Choice of a set  $\Phi$  containing the most important fault modes to diagnose:

1. By consulting the manufacturers' FMECA, select a suitable set of fault modes  $\Phi_m$  including probable fault modes of each component.
2. Develop mathematical and/or simulation models to evaluate fault mode severity by injection in the AOCS via simulation.
3. Collect simulation results and select a reduced set  $\Phi$  of the most critical mission fault modes contained in  $\Phi_m$ .

**Step 2:** Design of the Residual Generators and Robust Decision Functions for Fault Detection:

1. Design some residual generators which considers presence of uncertainty (disturbances and noises) in the model  $M$ .
2. Test, via simulation, the residues' sensitivity to faults.
3. Select the Residual Generator(s) which returns the most fault sensible residues.
4. Select some Decision Function(s) to emphasize the fault information and test it in several fault scenarios.
5. If disturbances, control actions and/or noise affects the Decision Function(s) response to fault and non-fault modes, design an Adaptive Threshold with robustness features. Otherwise, define a simple constant threshold.
6. Normalize the Decision Function(s) with the designed threshold.

**Step 3:** Design of a Structured Hypothesis Test for Fault Diagnosis:

1. Based on simulation results of the faulty AOCS, mount a binary symptom representation. Called here as **unified symptom representation**.
2. Generate a pattern for each scenario using some Decision Structure  $\gamma \in \Gamma$ .
3. Create  $S_n^1$  sets capable to explain each fault scenario.

4. Perform a SHT,  $\delta_i$ , having  $S_n^1$  and  $\Gamma$  as parameters.
5. The SHT  $\delta_i \in \Delta$  will be chosen if it can provide results with acceptable statistics compared with some specification (in terms of wrong diagnosis statements rate, normal mode declaration delay, conclusive diagnosis statements and etc).
6. This step is performed recursively, until obtain an acceptable  $\delta_i$ .

**Output:** The output is the SHT  $\delta$  adequate to the Fault Detection Scheme selected.

### 3. FDDS Design Methodology Applied to the MMP AOCS

The linear mathematical model of the nominal operating mode is in equation 1, where  $K_{TELDIX} = 7.5 \times 10^{-3}$  Nm/V is the reaction wheel gain and  $I_{sx} = 295.71 \text{ kg} \times \text{m}^2$ ,  $I_{sy} = 501.37 \text{ kg} \times \text{m}^2$  and  $I_{sz} = 364.82 \text{ kg} \times \text{m}^2$  are the satellite moments of inertia around the roll, pitch and yaw axis, respectively.

$$\begin{bmatrix} \dot{\phi} \\ \ddot{\phi} \\ \dot{\theta} \\ \ddot{\theta} \\ \dot{\psi} \\ \ddot{\psi} \end{bmatrix} = \begin{bmatrix} 0 & 1 & 0 & 0 & 0 & 0 \\ 0 & 0 & 0 & 0 & 0 & 0 \\ 0 & 0 & 0 & 1 & 0 & 0 \\ 0 & 0 & 0 & 0 & 0 & 0 \\ 0 & 0 & 0 & 0 & 0 & 1 \\ 0 & 0 & 0 & 0 & 0 & 0 \end{bmatrix} \begin{bmatrix} \phi \\ \dot{\phi} \\ \theta \\ \dot{\theta} \\ \psi \\ \dot{\psi} \end{bmatrix} + \begin{bmatrix} 0 & 0 & 0 \\ \frac{K_{TELDIX}}{I_{sx}} & 0 & 0 \\ 0 & \frac{K_{TELDIX}}{I_{sy}} & 0 \\ 0 & 0 & 0 \\ 0 & 0 & \frac{K_{TELDIX}}{I_{sz}} \end{bmatrix} \begin{bmatrix} V_{Rx} \\ V_{Ry} \\ V_{Rz} \end{bmatrix} \quad (1)$$

This model is used to simulate an off pointing maneuver by  $30^\circ$  in 180s. For this purpose, a suboptimal Linear Quadratic Tracking control law is used. The initial conditions are in equation 2.

$$\begin{bmatrix} \phi_0 \\ \dot{\phi}_0 \\ \theta_0 \\ \dot{\theta}_0 \\ \psi_0 \\ \dot{\psi}_0 \end{bmatrix} = \begin{bmatrix} 0^\circ \\ 0 \text{ rad/s} \\ 30^\circ \\ -0.001016 \text{ rad/s} \\ 0^\circ \\ 0 \text{ rad/s} \end{bmatrix} \quad (2)$$

Uncertainties are present in sensors (noise in star sensors and gyros), actuators (noise in control signal sent to the reaction wheels), and plant (external torques due to gravity gradient, parasite currents, aerodynamic drag and solar radiation pressure). Information about these uncertainties is summarized in Table 1.

Table 1. Components and its Fault Modes

Uncertainty	Component corrupted in three axis	Mathematical Model
Noise	Gyroscopes	White gaussian noise ( $\mu = 0$ and $\sigma = 10^{-5} \text{ rad/s}$ )
Noise	Reaction Wheels	White gaussian noise ( $\mu = 0$ and $\sigma = 10^{-3} \text{ Volts}$ )
Disturbance	Plant	Step (amplitude = $10^{-4} \text{ Nm}$ )

Since the scenario was described, the following three subsections will detail the application of the design methodology.

#### 3.1 Step 1 (Fault Modes Selection by severity judgement)

Based on the manufacturers' manual, [11], and on the AOCS Specifications Manual, [7], the following single fault modes in Table 2 were selected:

Table 2. Components and its Fault Modes

Index i	Component Name	Component Fault Modes	Component Type
g	Gyroscope	NF, CV, LV, OD, SD	Sensor
r	Reaction Wheel	NF, RA, RZ, HC, IV	Actuator

where the meanings are: NF = no fault, CV = constant value, LV = last value, OD = offset drift, SD = scale factor drift, RA = RPM above the limit, RZ = RPM near zero during a long period of time, HC = high armature current, and

IV = increasing velocity. Each component has four single fault modes, but the AOCS contains three reaction wheels and three gyroscopes in its nominal mode, summing twenty four single fault modes.

When prior knowledge or historical data is not available, fault models can be used to analyze each component fault mode and judge severity of the end-effects for the AOCS.

The fault models for each fault mode of the gyroscopes are in eqs. 3 to 7:

$$NF \rightarrow y(t) = \omega_n(t) \quad (3)$$

$$CV \rightarrow y_{F_1}(t) = \begin{cases} \theta Y_o(t) + f_{1,1}(t)Y_o(t), & \text{if } t_{f_{1,1}} \leq t \leq t_{f_{1,1}} + d_{f_{1,1}} \\ f_{1,2}(t), & \text{if } t_{f_{1,2}} \leq t \leq t_{f_{1,2}} + d_{f_{1,2}} \\ f_{1,3}(t), & \text{if } t_{f_{1,3}} \leq t \leq t_{f_{1,3}} + d_{f_{1,3}} \end{cases} \quad (4)$$

$$LV \rightarrow y_{F_2}(t) = \theta Y_o(t) - p(d_{f_2})\theta Y_o(t) + p(d_{f_2}) \int_{t_{f_2}}^{t_{f_2}+d_{f_2}} \varepsilon^{-1} p(\varepsilon) Y_o(t) dt : \varepsilon \ll 1 \quad (5)$$

$$OD \rightarrow y_{F_3}(t) = Y_o(t) \{ \theta + K_o(t) [1(t - t_{f_3}) - 1(t - t_{f_3} - d_{f_3})] \} \quad (6)$$

$$SD \rightarrow y_{F_4}(t) = \{ [1(t - t_{f_4}) - 1(t - t_{f_4} - d_{f_4})] K_e(t) + 1 \} Y_o(t) : K_e(t, t_{f_4}) = \begin{cases} 0, & \text{if } t < t_{f_4} \\ (t - t_{f_4})\beta, & \text{if } t \geq t_{f_4} \end{cases} \quad (7)$$

where  $p(\rho) = [1(t - t_{f_2}) - 1(t - t_{f_2} - \rho)]$ ,  $t_{f_i}$  is the time of occurrence of the fault  $i$ ,  $d_{f_i}$  is the duration of the fault  $i$ ,  $f_{1,1} = -\theta$ ,  $f_{1,2} = \text{maximum\_scale\_value}$ ,  $f_{1,3} = \text{random\_value}$ ,  $Y_o(t)$  is the true input value,  $\theta$  is a measurement degradation parameter,  $\omega_n(t)$  is the noise corrupted angular velocity measurement, and CV has three different modes for the same fault.

The fault models for the gyro were developed in the time domain. Note that the fault models for the gyro expresses only effects on measurements, but not changes in dynamic relations inside the sensor itself.

The fault models for each fault mode of the reaction wheels are in eqs. 8 to 12:

$$NF \rightarrow T(s) = \frac{K}{1 + T_i s} U_e(s) \quad (8)$$

$$RA \rightarrow T(s) = K \left[ U_e(s) \frac{1 - e^{-t_{f_5}s} + e^{-(t_{f_5}+d_{f_5})s}}{s} + \frac{e^{-t_{f_5}s} - e^{-(t_{f_5}+d_{f_5})s}}{s} f_5 \right] \text{ and } \Omega(s) = T(s) \cdot \frac{1}{I_r} \cdot \frac{1}{s} \quad (9)$$

$$RZ \rightarrow T(s) = K \left[ U_e(s) \frac{1 - e^{-t_{f_5}s} + e^{-(t_{f_5}+d_{f_5})s}}{s} \right] \quad (10)$$

$$HC \rightarrow T(s) = K U_e(s) - \frac{e^{-t_{f_7}s} - e^{-(t_{f_7}+d_{f_7})s}}{s} \alpha U_e(s) \quad (11)$$

$$IV \rightarrow T(s) = K U_e(s) + \frac{e^{-t_{f_8}s} - e^{-(t_{f_8}+d_{f_8})s}}{s} f_8 \text{ and } \Omega(s) = T(s) \cdot \frac{1}{K} \cdot \frac{1}{s} \quad (12)$$

where  $T(s)$  is the reaction wheel torque,  $K$  is the gain,  $T_i$  is the time constant,  $\Omega(s)$  is the velocity,  $I_r$  is the reaction wheel moment of inertia,  $\alpha$  is a degradation factor,  $U_e(s)$  the input voltage, and  $f_i$  is the amplitude of the  $i^{th}$  fault.

The fault models for the reaction wheel were developed in frequency domain. Note that the fault models for the reaction wheel consider changes in dynamic relations inside the actuator itself.

The total model of the system to be diagnosed (the AOCS) is the union of all relations describing the components (equations 3 to 12). As done for defining fault modes for the components, we can define system fault modes by selecting them by severity judgement. This procedure is based on an analysis of the system behavior by simulating the faulty scenarios (modeled in equations 3 to 12). The single fault modes are injected on an environment with noise corrupted gyros, reaction wheel control signals, and disturbances on the plant.

The simulations showed that all twenty four fault modes are harmful to the system: in certain cases these scenarios do not caused instability, but matching of specifications was not possible. In general, this behavior depends on fault in amplitude, the highest ones caused instability. All faults could cause instability; then they were judged as having the same severity and necessity to be detected and diagnosed. Then all single fault modes in Table 1 have to be promptly detected and diagnosed.

### 3.2 Step 2 (Design of the Residual Generators and Robust Decision Functions for Fault Detection)

This step is contained on the step 5 of Figure 1. The overall structure of the FDD method can be subdivided in two parts: Fault Detection and Fault Diagnosis. In this step 2, Fault Detection is of concern.

In the field of control theory, the literature on fault detection has mostly been focused on the problem of residual generation, which leads to the structure illustrated in Figure 2.

Where the information provided by the measurements are combined with previous knowledge (mathematical model) to generate residuals, a decision function is applied to evidence the fault presence subsequently. The output of this fault detection scheme is mostly affected by noise, disturbances and modeling errors. It implies that the application of the threshold logic can generate erroneous symptoms when uncertainty is present.

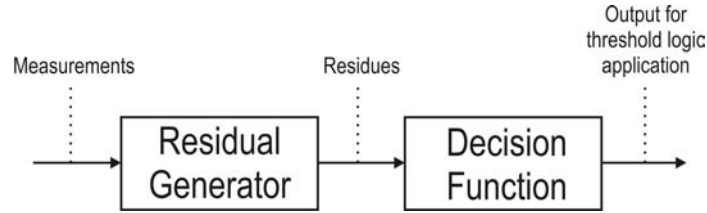


Figure 2. General structure for Fault Detection.

The techniques used to detect faults in gyros are: Kalman filter innovations (Residual Generator, equation 13) and Sequential Probability Ratio Test (Decision Function, equation 14).

$$r_g(k) = \bar{K} [y(k) - \hat{\omega}(k|k-1)] \quad (13)$$

$$T_g(k) = \sum_{k=k_0}^{k_0+N} r^2(k) \quad (14)$$

On the other hand, the techniques used to detect faults in reaction wheels are: structured residuals (Residual Generator, equation 15) and Absolute Value Calculation (Decision Function, equation 16).

$$\begin{bmatrix} R_{1r}(s) \\ R_{2r}(s) \\ R_{3r}(s) \end{bmatrix} = \begin{bmatrix} \frac{K_m}{J} I_n(s) - sK_{I_a} \Omega_n(s) \\ -\frac{K_m}{J} U(s) + s\Omega_n(s) \\ -sU(s) + \frac{s}{K_{I_a}} I_n(s) \end{bmatrix} \frac{1}{T_i s + 1} \quad (15)$$

$$\begin{bmatrix} T_{1r}(k) \\ T_{2r}(k) \\ T_{3r}(k) \end{bmatrix} = \begin{bmatrix} |r_{1r}(k)| \\ |r_{2r}(k)| \\ |r_{3r}(k)| \end{bmatrix} \quad (16)$$

Note that the techniques are different but the architecture is the same, Residual Generator followed by a Decision Function. Only one residual is evaluated for each gyro, and three other residues are evaluated for each reaction wheel. Equation 15 shows that the reaction wheel residues are filtered by a low pass filter with the time constant equals to that of the reaction wheel motor.

To avoid missed and false alarms propagation since detection, some robustness questions arise in FDD. The robustness issue is hardly integrated as a part of the design process for the Decision Functions. Methods to achieve and analyze robustness have been extensively studied, see [4] and [5]. There are experimental results showing the advantage of this robustness approach as an additional design step in adjusting and compensating the original Decision Function designed, see [6].

Specially in this work, robustness is achieved via normalization. It mainly consists in designing an adaptive threshold, according to [10] described by the more general form in equation 17.

$$J_{adp} = c_1 W(u, y) + c_2 \quad (17)$$

Since  $W(u, y)$  is some measure of the model uncertainty present, to set an adaptive threshold is equivalent to normalize the Decision Function. After some Decision Function ( $T(k)$ ) calculation, it will be compared with a threshold to generate some symptom. Equation 18 shows the normalization reasoning due to [10].

$$T(k) \geq J_{adp} \rightarrow \frac{T(k)}{c_1 W(u, y) + c_2} \geq 1 \quad (18)$$

The suitable adaptive thresholds for the gyros and reaction wheel Decision Functions are of the general form given in Table 3.

Table 3. Adaptive thresholds' general form parameters

Component	$c_1 W(u, y)$	$c_2$
$\underline{g}$	$J_1^1  V_{rx}(k)  + J_2^1  V_{ry}(k)  + J_3^1  V_{rz}(k) $	$J_r^1$
r	0	$J_g^1$

Where  $J^i$  are constants, and  $V_r(k)$  are reaction wheel voltage control signals.

Now, it is possible to evaluate the normalized Decision Function to generate unified symptoms representation. Unified symptoms representation consists in a technique to group information available from fault detection and prepare it for diagnostics. As can be seen, different techniques are used to detect faults in different components; in other words, different Fault Detection Systems had been applied.

But the diagnostics consider system fault modes, not single component fault modes; then it is necessary to apply some technique capable of unifying information coming from the two Fault Detection Systems; and interface it with the Fault Diagnosis System.

Each normalized Decision Function generates a corresponding unified symptom, but it could be different too. This unified symptom representation is generated by threshold evaluation like equation 19.

$$s_i = \begin{cases} 0, & \text{if } T_i^{norm}(k) < 1 \\ 1, & \text{if } T_i^{norm}(k) \geq 1 \end{cases} \quad (19)$$

These binary variables (unified symptoms) are used directly in Structured Hypothesis Testing (SHT). A tool to design the SHT is the Decision Structure, which relates some possible symptoms with the most probable system fault modes.

### 3.3 Step 3 (Design of a Structured Hypothesis Test for Fault Diagnosis)

The Fault Detection is interfaced with the Fault Diagnosis through a Decision Structure. It happens because the evaluation of the Decision Functions generate symptoms. These symptoms are used to construct a Decision Structure. Once a Decision Structure is constructed, some logic is applied in order to classify the fault mode present at the system. This last step is the Fault Diagnosis. An example of a Decision Structure is the Table 4.

Table 4. FDDS Decision Structure

	NF	CV	LV	OD	SD	RA	RZ	HC	IV	Decision Function related to
$s_1$	0	×	×	×	×	0	0	0	0	roll gyro
$s_2$	0	×	×	×	×	0	0	0	0	pitch gyro
$s_3$	0	0	0	0	0	0	0	0	0	yaw gyro
$s_4$	×	0	×	0	0	0	0	0	0	pitch star sensor
$s_5$	0	0	0	0	0	×	×	×	×	pitch reaction wheel (residue 1)
$s_6$	0	0	0	0	0	×	×	0	×	pitch reaction wheel (residue 2)
$s_7$	0	0	0	0	0	×	×	0	0	pitch reaction wheel (residue 3)

In Table 4, a 0 at the  $i^{th}$  row and  $j^{th}$  column signifies that the  $i^{th}$  symptom do not manifests itself for the  $j^{th}$  fault mode. A × at the  $i^{th}$  row and  $j^{th}$  column signifies that the  $i^{th}$  symptom could or not manifest itself for the  $j^{th}$  fault mode. A 1 at the  $i^{th}$  row and  $j^{th}$  column signifies that the  $i^{th}$  symptom manifest itself for the  $j^{th}$  fault mode. The decision structure at Table 3 do not uses 1's, only ×'s to denote a possible symptom manifestation. This is a characteristic which could improve robustness in a speculative Fault Diagnosis System, concept which will be clarified in the following.

Based on symptoms manifestation and Decision Structure relations, a SHT is employed. Each individual hypothesis test will be named as  $\delta_i(x)$  and returns an individual diagnosis statement. Then a diagnosis system consists on a set of hypothesis tests,  $\delta_1(x)$  to  $\delta_n(x)$ , and a decision logic specified by the Decision Structure from which diagnosis statements are generated.

The test  $\delta_i(x)$  is a function of the measurements  $y$  and the control signals  $u$ , i.e.  $\delta_i(x) = \delta_i([u \ y])$ . The null hypothesis to the  $i^{th}$  hypothesis test, called  $H_i^0$ , says that the fault mode present at the system belongs to the set  $S_i^0$  of fault modes. An alternative hypothesis  $H_i^1$  says that the present fault mode do not belongs to  $S_i^0$ . If the hypothesis  $H_i^0$  is rejected, then  $H_i^1$  is accepted. In other words, the present fault mode cannot belong to  $S_i^0$ , it may belong to another set,  $S_i^1$ .

Consider  $F_a$  as the actual system fault mode. At the  $i^{th}$  hypothesis test, the null hypothesis and the alternative hypothesis can be written as follows:

- $H_i^0 : F_a \in S_i^0 \longrightarrow$  "some fault mode in  $S_i^0$  can explain the measured data"
- $H_i^1 : F_a \notin S_i^0 \longrightarrow$  "no fault mode in  $S_i^0$  can explain the measured data"

All the single diagnosis statements have information about which system fault mode can explain the data. To obtain the final diagnosis statement  $S$ , we have to combine information contained inside each single diagnosis statement,  $S_i$ . The  $S_i^1$  sets for evaluation during SHT where defined as follows in Table 5.

Table 5. Sets to form a diagnosis statement at each single hypothesis test

$i$	$S_i^1$
$\delta_{gx}$	{VCY, UVY, DOY, DEY}
$\delta_{gy}$	{VCY, UVY, DOY, DEY}
$\delta_{gz}$	{}
$\delta_{ey}$	{SF, UVY}
$\delta_{rx}$	{RLY, RZY, CAY, VAY}
$\delta_{ry}$	{RLY, RZY, VAY}
$\delta_{rz}$	{RLY, RZY}

Through the set representation, this combination is done by means of intersection operation, i.e., the final diagnosis statement,  $S$ , is formed according to eq. 20:

$$S = \bigcap_{i=1}^n S_i \tag{20}$$

The decision logic of the diagnosis system can be viewed as a simple intersection algorithm. And this is the third and last step performed to design the FDDS. The next section describes the FDD algorithm, focus of this work.

#### 4. The Algorithm

Previously, the methods and techniques were described. Figure 3 offers an FDDS scheme overview, which shows the relations of the entire procedure.

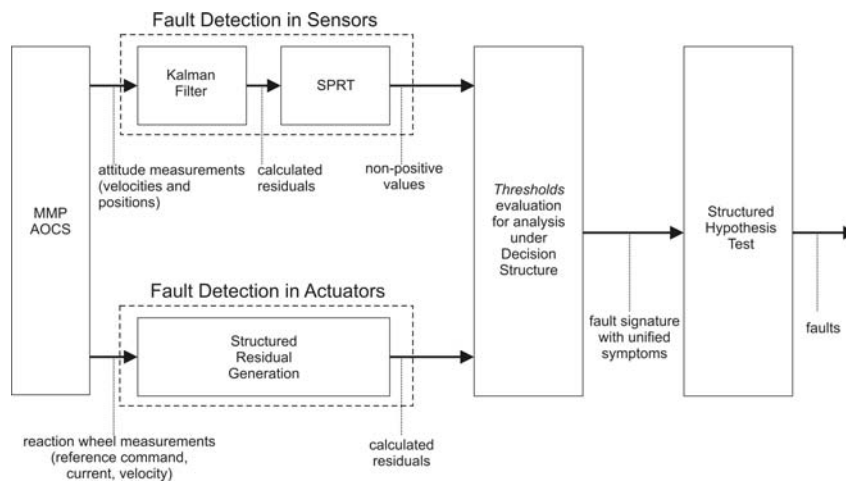


Figure 3. FDDS scheme overview.

Note that the main source of information is the AOCs: This information is acquired from the attitude sensors (gyros and star sensors), controller (control signals) and actuators (reaction wheel sensors of current and velocity). These signals are processed within a Fault Detection Scheme by different techniques following the same method. The information coming from this Fault Detection Scheme is unified to be treated in a common structure; this unification is a result of a threshold evaluation to generate unified symptoms representation. Each threshold evaluation gives a specific symptom value; all the symptoms can be stored into a vector which is called fault signature. This fault signature can be explained by one or more fault modes, but this is a task employed by the SHT. The SHT offers a set of the possible fault modes which can explain the measured data from de AOCs. This result is called **diagnosis statement**.

The procedure has to be executed continuously by the ACDH (Attitude Control and Data Handling) Subsystem. An algorithm is proposed in this work aiming to execute this task. Figure 4 shows a flowchart which illustrates the functioning of this algorithm.

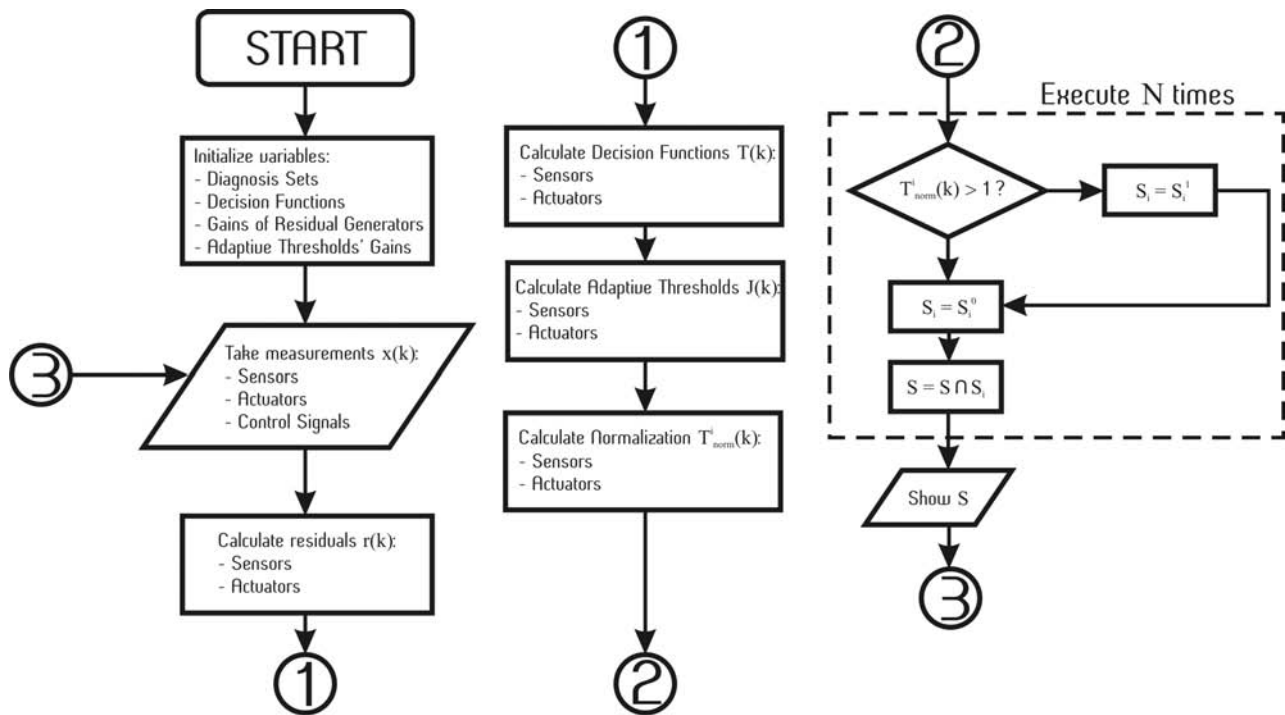


Figure 4. Flowchart of the FDD algorithm

In the algorithm (see Figure 4), some variables are firstly initialized. These variables are the Diagnosis Sets  $S_i^0$  and  $S_i^1$  which are vector valued, Decision Functions' parameters like width of the moving window of the SPRT (Sequential Probability Ratio Test), gains of Residual Generators like Kalman Filter Gain  $\bar{K}$  and parameters of the equation 17, gains of Adaptive Thresholds like those in Table 3 and other variables related to implementation issues in some programming language.

Subsequently, a single sample of each signal is taken, over these information a residual calculation is applied followed by decision functions calculation, adaptive threshold calculation and normalization. Now the information is ready to be used in SHT, which used the result of threshold evaluation of each normalized decision function to mount a diagnosis statement and show it to the monitor.

This monitor could be a ground operator or an automatic reconfiguration system. Once developed, this algorithm can be used for virtual time simulation, real time simulation and hardware-in-the loop simulation before code embedding for the ACDH. These first steps were employed for verification and validation and described in previous works, [9] and [1]. However, some tests must be made before extending and adapting the algorithm to the AOCS of the engineering model of the MMP Satellite at the nominal operation mode.

Section 5 shows some results of the application of the methods, techniques and algorithm to the case under study.

## 5. Some Results

When some fault mode  $F_a$  is applied to the pitch gyro, this fault is called  $F_a Y$ , and the same form for reaction wheels and another gyros. Then the fault  $LV$  applied to the pitch gyro is called  $LVY$ , etc. This nomenclature is adopted to show some results. See, for example, Table 6.

The results shown at Table 6 explicitly can lead to the conclusion of fault in sensors, not in actuators. It is true, but the isolation is not perfect, since nine different fault modes could explain the data measured. This results could be improved, but the FDDS concerns with other 15 faults. Adjustments in the Decision Functions, Adaptive Thresholds, Decision Structure, etc. could lead to better results in detection and diagnosis of this fault mode ( $LVY$ ); but it could not be the better choice for the other 23 fault modes. Note that the fault modes neglected at Table 6 achieved 0% of diagnosis occurrence. Another results for the algorithm with the same tuned parameters are in Table 7.

The results in Table 7 are better than those in Table 6 under the point of view of correct diagnosis occurrence. But detection delays and  $NF$  mode declaration are completely different, see Table 8. This is a multi-purpose problem.

Table 6. FDDS results in presence of fault mode *LVY*

Mode	Correct diagnosis occurrence	Mode	Correct diagnosis occurrence
<i>NF</i>	35.56%	<i>SDY</i>	64.30%
<i>CVX</i>	64.30%	<i>CVZ</i>	64.30%
<i>CVY</i>	64.30%	<i>LVZ</i>	64.44%
<i>LVY</i>	64.30%	<i>ODZ</i>	64.44%
<i>ODY</i>	64.30%	<i>SDZ</i>	64.30%

Table 7. FDDS results in presence of fault mode *CVZ*

Mode	Correct diagnosis occurrence	Mode	Correct diagnosis occurrence
<i>NF</i>	05.47%	<i>LVZ</i>	94.28%
<i>CVX</i>	05.22%	<i>ODZ</i>	94.28%
<i>ODX</i>	05.22%	<i>SDZ</i>	05.22%
<i>CVZ</i>	94.28%		

Table 8. Other parameter to compare results in tables 6 and 7.

	Detection delay	<i>NF</i> mode declaration delay
<b>Table 6 results</b>	15.6s	1.9s
<b>Table 7 results</b>	0.2s	275.3s

The same problem occurs when FDDS is applied to the case of fault in reaction wheels. Table 9 shows results when fault mode *IVX* is injected, when detection delay was 3.4s and *NF* mode declaration delay was 0s.

Table 9. FDDS results in presence of fault mode *IVX*

Mode	Correct diagnosis occurrence	Mode	Correct diagnosis occurrence
<i>NF</i>	33.90%	<i>HGX</i>	66.10%
<i>RAX</i>	66.10%	<i>IVX</i>	66.10%
<i>RZX</i>	66.10%		

All results for FDDS applied to the reaction wheel achieved perfect isolation, but conclusive diagnostics for better identification are rare.

As said before, faults applied to actuators and sensors affect stability of the entire AOCS. But the detection delays are sufficient in such a way that reconfiguration of control law is feasible.

## 6. Concluding Remarks

Robustness, promptness in detection, correctness in diagnosis statements and thresholds selection are always of special interest in FDD. This work is not different in concerning with these aspects.

Results in Table 6 and 7 shown problems due to coupling, which can be seen as predictable when we look at the equation 21.

$$\begin{bmatrix} \dot{\phi} \\ \dot{\theta} \\ \dot{\psi} \end{bmatrix} = \begin{bmatrix} \omega_{sx} + \frac{(\sin \phi \times \sin \theta \times \omega_{sy} + \cos \phi \times \sin \theta \times \omega_{sz} + \omega_0 \sin \psi)}{\cos \theta} \\ \cos \phi \times \omega_{sy} - \sin \phi \times \omega_{sz} + \omega_0 \cos \psi \\ \frac{(\sin \phi \times \omega_{sy} + \cos \phi \times \omega_{sz} + \omega_0 \sin \theta \times \sin \psi)}{\cos \theta} \end{bmatrix} \quad (21)$$

Threshold selection affect enormously on the FDDS' performance, see Figure 5, where  $\theta$  is the fault amplitude,  $J$  is the threshold and  $R(\theta, J)$  is the missed alarm rate.

The exponential behavior is present when relating delays (detection and *NF* declaration) and missed alarms rate; i.e., big detection delays corresponds to very small missed alarm rates and *mutatis mutandis* for the *NF* declaration case.

Robustness was achieved here using normalization. This is a good alternative, but systematic methods have to be studied to design an adaptive threshold which improves FDDS robustness.

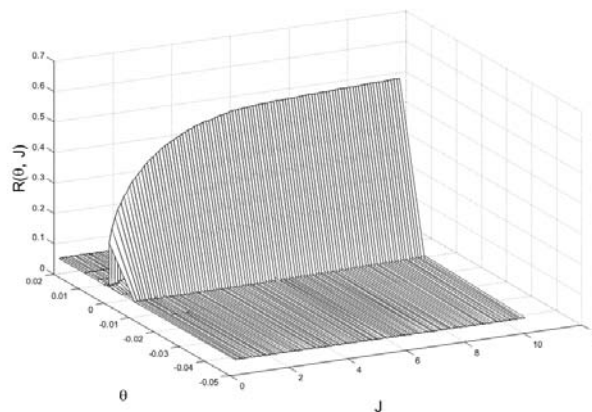


Figure 5. Missed alarm rate for  $CVX$

Finally, we can conclude that the results were satisfactory because many faults were considered in the presence of uncertainties.

## 7. ACKNOWLEDGEMENTS

Thanks to the friends of LAI at CEFET Campos and LABSIM2 at INPE/DMC for comments, suggestions and discussions. The first author thanks CEFET Campos for supporting him and the Laboratory for Automation and Instrumentation-LAI where part of this research was done. The second author thanks INPE for supporting him and the Laboratory for Computational Environments for Simulation, Identification, and Modeling-LABSIM2 of AOCS where part of this research was done.

## 8. REFERENCES

- Amorim III, F.C. and Souza, M.L.O., 2007, "A Parallel/Distributed Simulator Applied to the Multi-Mission Platform Satellite Attitude Control", submitted to Proceedings of the 19th International Congress of Mechanical Engineering, Brasilia, Brazil.
- Blanke, M., Kinnaert, M., Lunze, J., Staroswiecki, M., Schröder, J., 2006, "Diagnosis and Fault-Tolerant Control", Springer.
- Bøgh, S.A. and Blanke, M., 1997, "Fault-Tolerant Control - A Case Study of the Ørested Satellite", IEEE Colloquium on Fault Diagnosis in Process Systems, 21 Apr., Pages 11/1.
- Chen, J. and Patton, R.J., 1999, "Robust Model-Based Fault Diagnosis for Dynamic Systems", Kluwer Academic Publishers.
- Frisk, E. and Nielsen, L., 1999, "Robust Residual Generation for Diagnosis Including a Reference Model for Residual Behavior", IFAC.
- Höfling, T. and Isermann, R., 1996. "Fault detection based on adaptive parity equations on single-parameter tracking", Control Eng. Practice 4(10), 1361-1369.
- INPE, 2001. "Multi-Mission Platform Attitude Control and Data Handling (ACDH) Subsystem Specification", Instituto Nacional de Pesquisas Espaciais, A822700-SPC-001/05, São José dos Campos, SP, Brazil.
- Krysanter, M. and Nyberg, M., 2003, "Combining AI, FDI, and Statistical Hypothesis Testing in a Framework for Diagnosis", Proceedings of IFAC Safeprocess'03, Washington, USA.
- Leite, A.C. and Souza, M.L.O., 2007, "A MRAC Structure for HiL Reaction Wheel Emulation in a Satellite Attitude and Orbit Control System Simulation under a Faulty Environment", Submitted to the IFAC Symposium on Systems, Structure and Control - SSSC07, Foz do Iguaçu, Brazil.
- Nyberg, M., 1999, "Model Based Fault Diagnosis Methods, Theory, and Automotive Engine Applications", PhD Thesis, Linköping University, Department of Electrical Engineering.
- TELDIX, 2005, "Technical Description", RSI-12-75/601.

## 9. Responsibility notice

The authors are the only responsible for the printed material included in this paper